

Supporting Information

Construction of nickel and sulfur co-existed carbon nanotubes derived from hydrogen-bonded organic framework for efficient biomass electrooxidation

*Yuting Zhang,^a Junhua Kuang,^a Jia Yu,^{*a} Yangyang Dong,^a Jiaran Li,^a Tianwei Xue,^a Jing Wu,^a Junchi Ma,^a Jinlong Wan,^a Shiping Zeng,^a Yong Sun,^a Yue-Jiao Zhang,^a Jin-Chao Dong,^a Li Peng,^{*a} Shuliang Yang^{*a}, and Jian-Feng Li^{*a}*

a. College of Energy, College of Chemistry and Chemical Engineering, Xiamen University, Xiamen 361102, Fujian, PR China. E-mail: yujia@xmu.edu.cn; li.peng@xmu.edu.cn; ysl@xmu.edu.cn; li@xmu.edu.cn

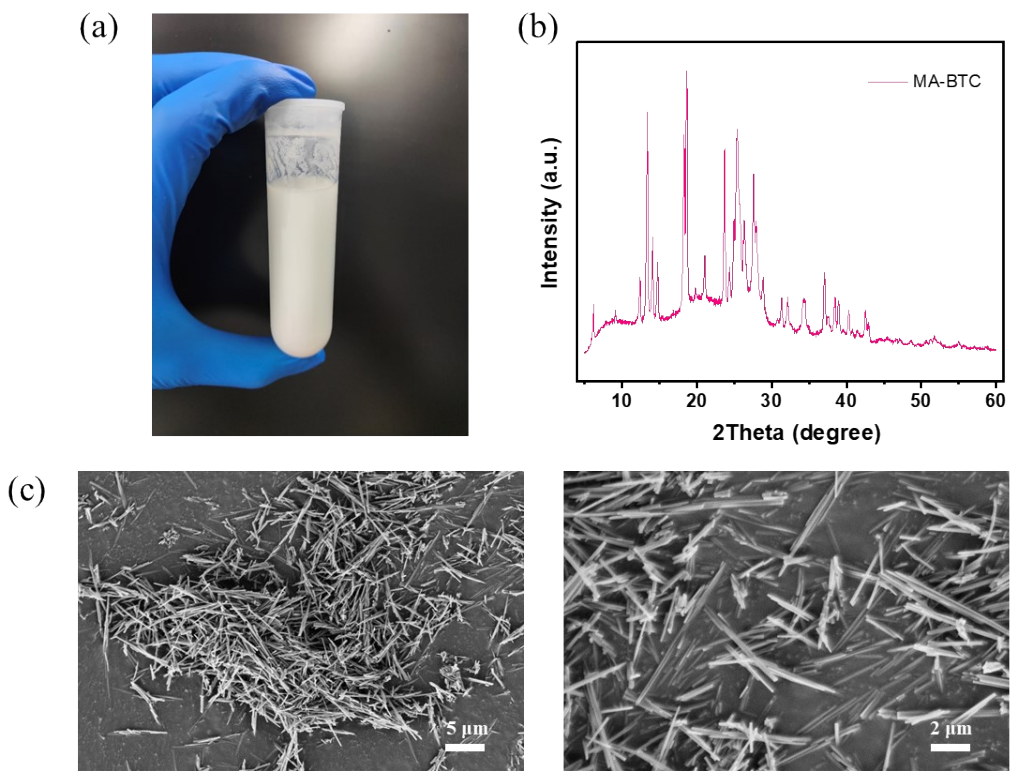


Figure S1. (a) Digital photo of MA-BTC HOFs in 35 mL of methanol. It was ultrasonicated for 2 h and then kept still for 20 min. XRD pattern (b) and SEM images (c-d) of the synthesized MA-BTC precursor.

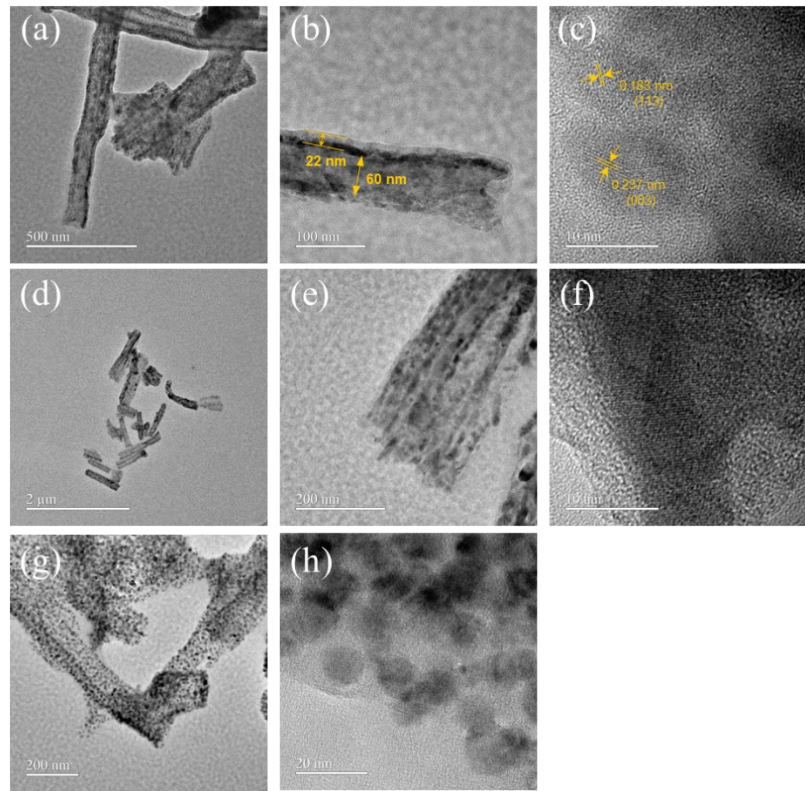


Figure S2. TEM images of (a, b) $\text{Ni}_{2.4}\text{S}_{0.1}@\text{CNTs}$, (d, e) $\text{NiSO}_4@\text{CNTs}$, and (g) $\text{Ni}(\text{NO}_3)_2@\text{CNTs}$. HRTEM images of (c) $\text{Ni}_{2.4}\text{S}_{0.1}@\text{CNTs}$, (f) $\text{NiSO}_4@\text{CNTs}$, and (h) $\text{Ni}(\text{NO}_3)_2@\text{CNTs}$.

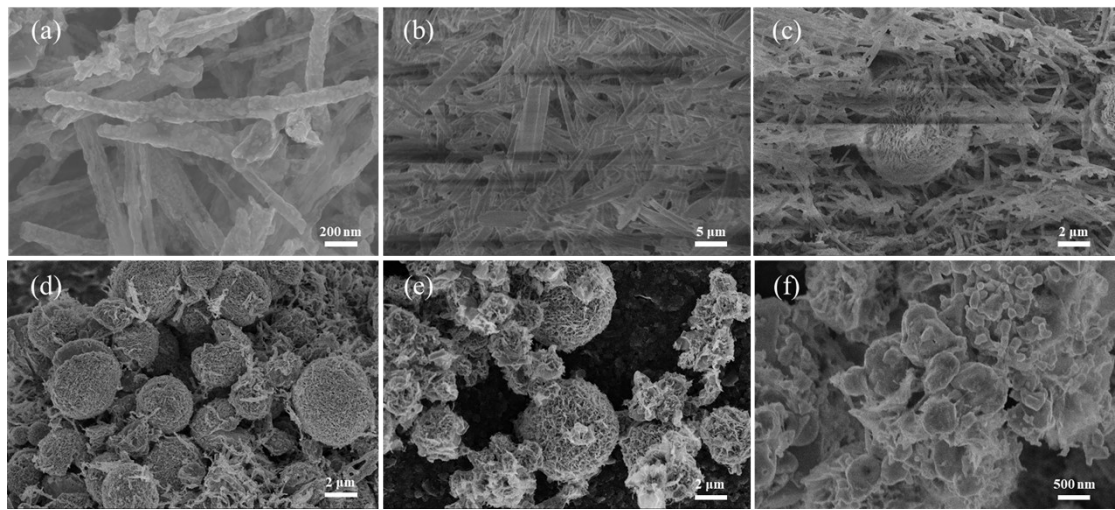


Figure S3. SEM images of the catalysts with varying amount of sulfur contents: (a) without additional sulfur; (b) 0.1 mmol of thiourea; (c) 0.3 mmol of thiourea; (d) 0.6 mmol of thiourea; (e) 1.2 mmol of thiourea, and (f) 1.8 mmol of thiourea.

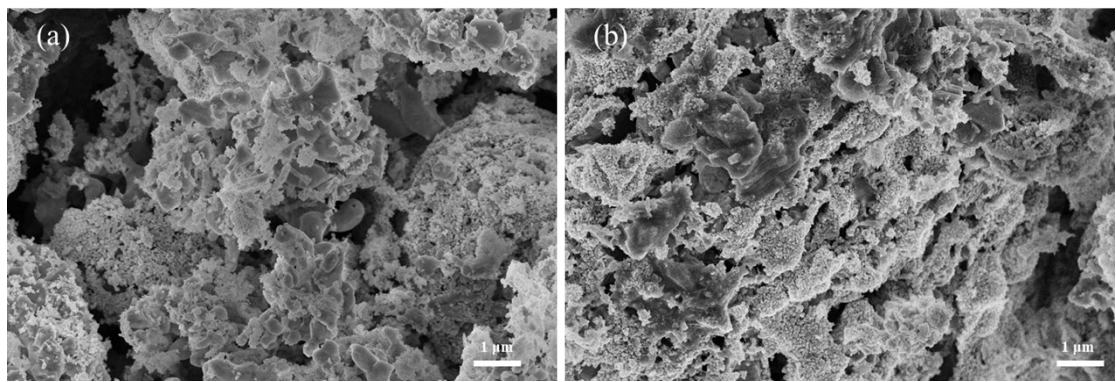


Figure S4. SEM images of the catalysts with excessively used NiSO_4 : (a) 3.0 mmol of NiSO_4 and (b) 3.6 mmol of NiSO_4 .

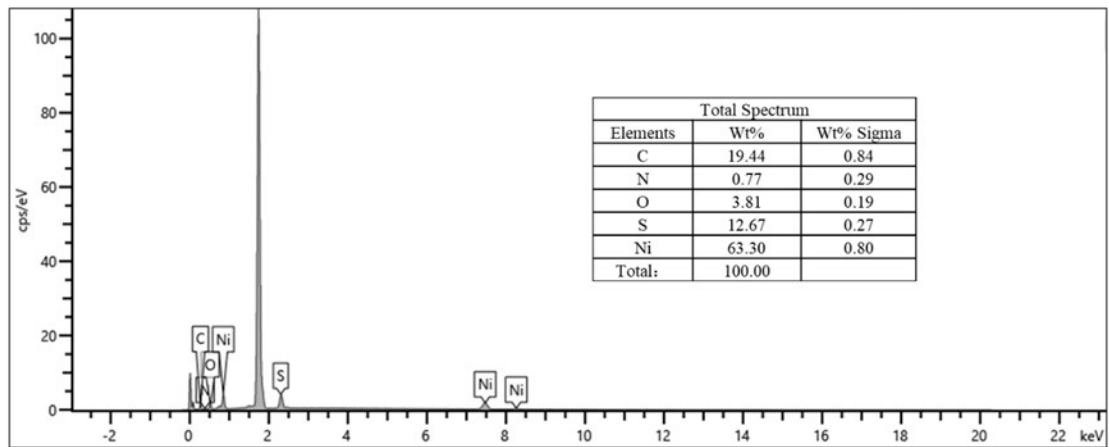


Figure S5. SEM-EDS spectrum for $\text{Ni}_{2.4}\text{S}_{0.1}@\text{CNTs}$.

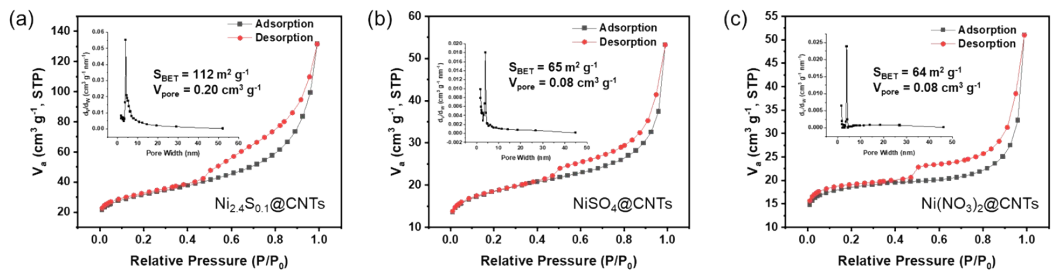


Figure S6. N_2 adsorption-desorption isotherms at 77 K of (a) $\text{Ni}_{2.4}\text{S}_{0.1}@\text{CNTs}$, (b) $\text{NiSO}_4@\text{CNTs}$, and (c) $\text{Ni}(\text{NO}_3)_2@\text{CNTs}$.

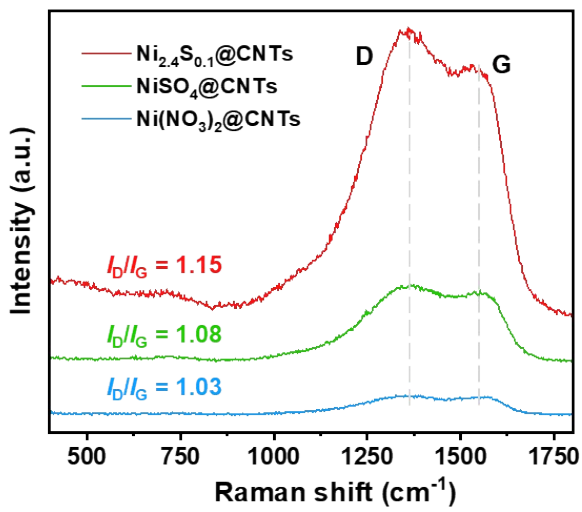


Figure S7. Raman spectra of $\text{Ni}_{2.4}\text{S}_{0.1}\text{@CNTs}$, $\text{NiSO}_4\text{@CNTs}$, and $\text{Ni}(\text{NO}_3)_2\text{@CNTs}$.

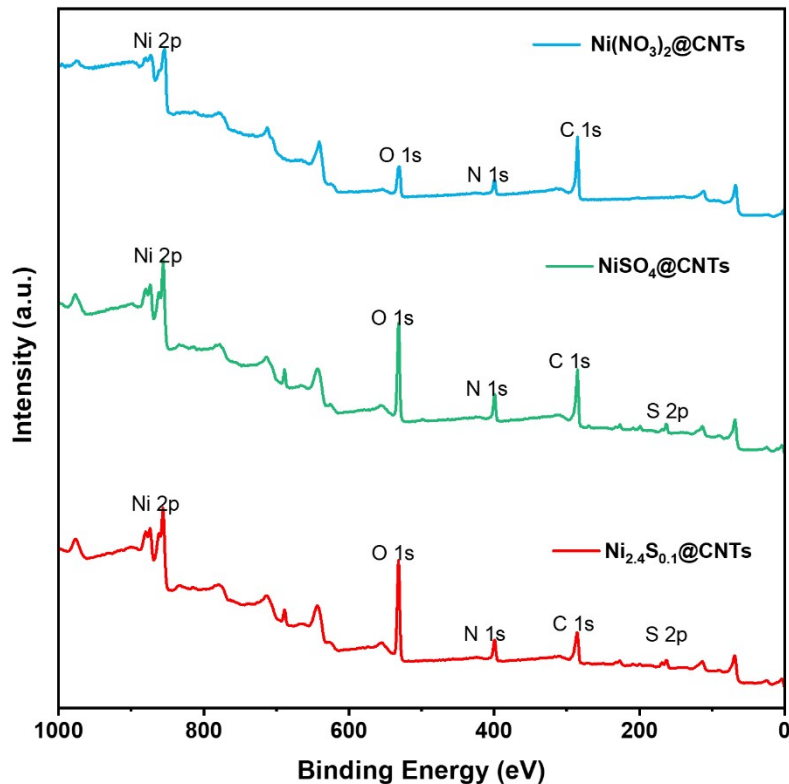


Figure S8. XPS survey scan spectra of $\text{Ni}(\text{NO}_3)_2@\text{CNTs}$ (blue), $\text{NiSO}_4@\text{CNTs}$ (green), and $\text{Ni}_{2.4}\text{S}_{0.1}@ \text{CNTs}$ (red).

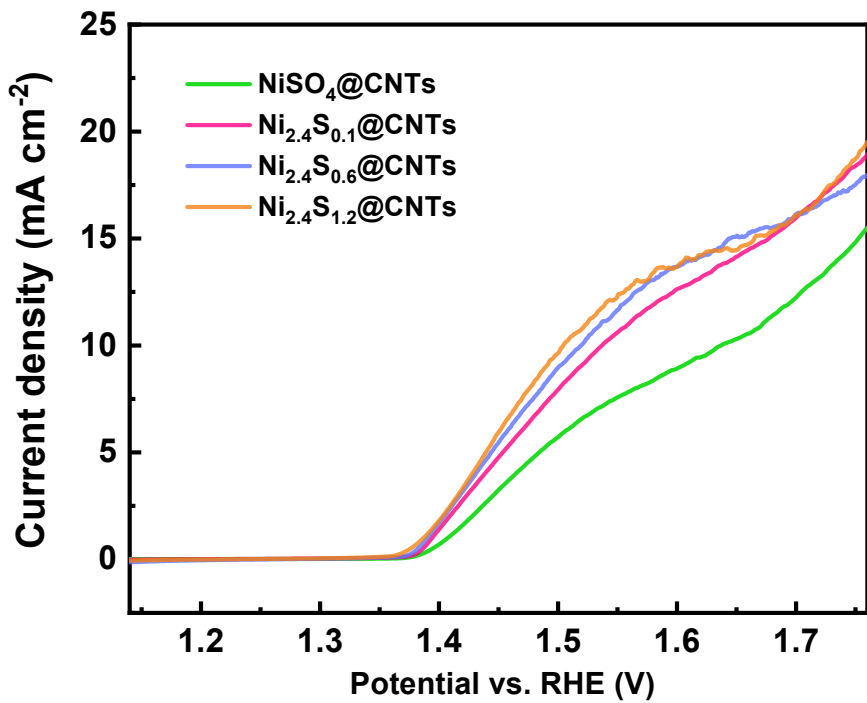


Figure S9. LSV curves of Ni_{SO₄}@CNTs (green), Ni_{2.4}S_{0.1}@CNTs (carmine), Ni_{2.4}S_{0.6}@CNTs (purple), and Ni_{2.4}S_{1.2}@CNTs (orange) in 0.1M KOH with 10 mM HMF.

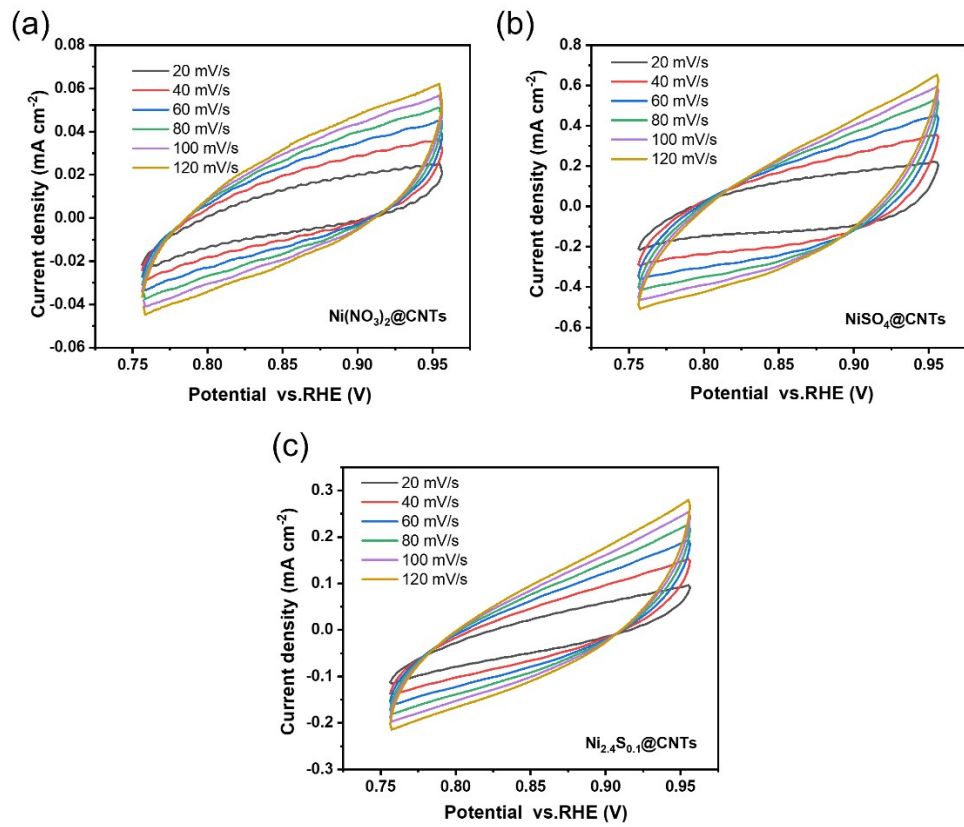


Figure S10. Cyclic voltammetry curves of: (a) $\text{Ni}(\text{NO}_3)_2@\text{CNTs}$, (b) $\text{NiSO}_4@\text{CNTs}$, and (c) $\text{Ni}_{2.4}\text{S}_{0.1}@ \text{CNTs}$ with different scan rates.

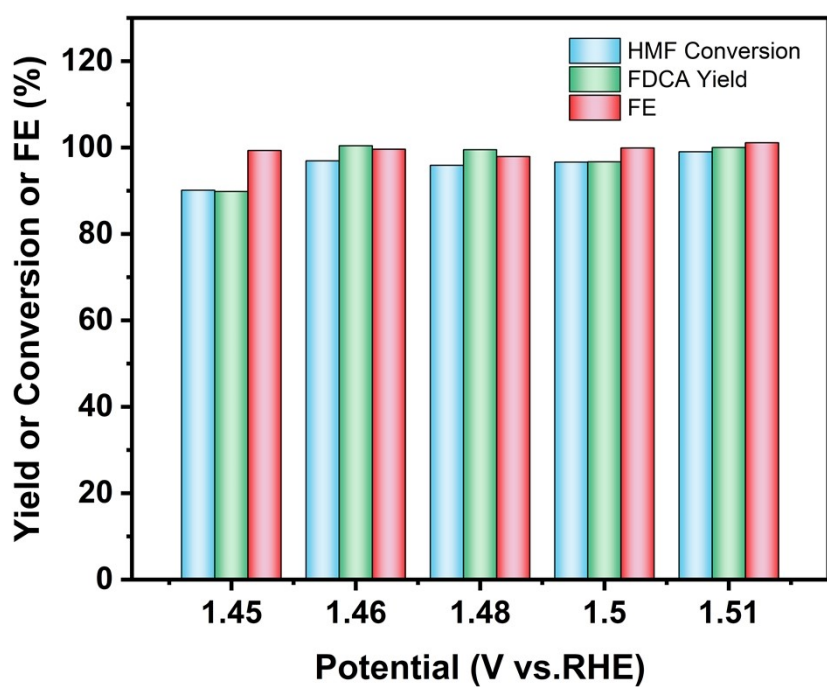


Figure S11. HMF conversion, FDCA yield and FE of $\text{Ni}_{2.4}\text{S}_{0.1}@\text{CNTs}$ at different potentials in 0.1 M KOH with 10 mM HMF.

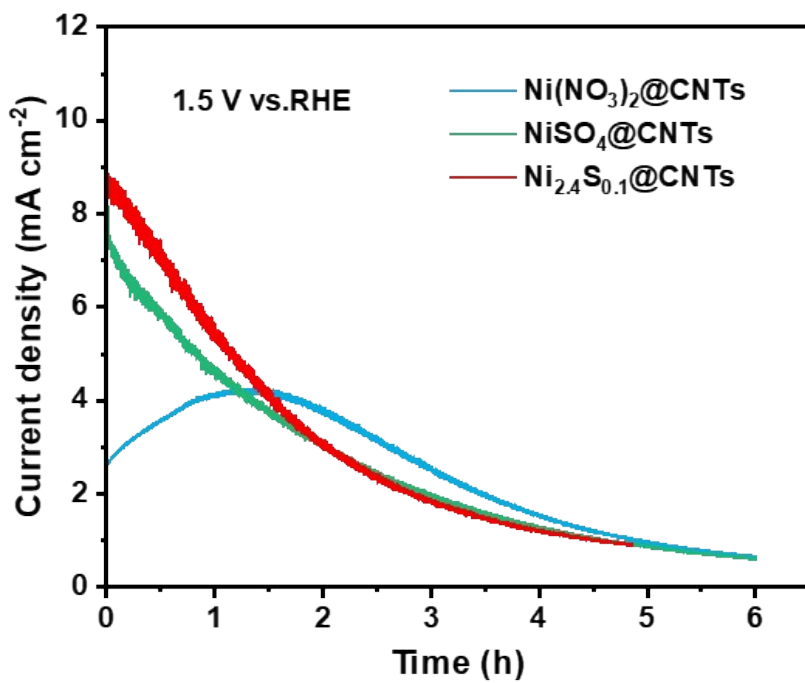


Figure S12. Current-time plots for different catalysts derived from chronoamperometry.

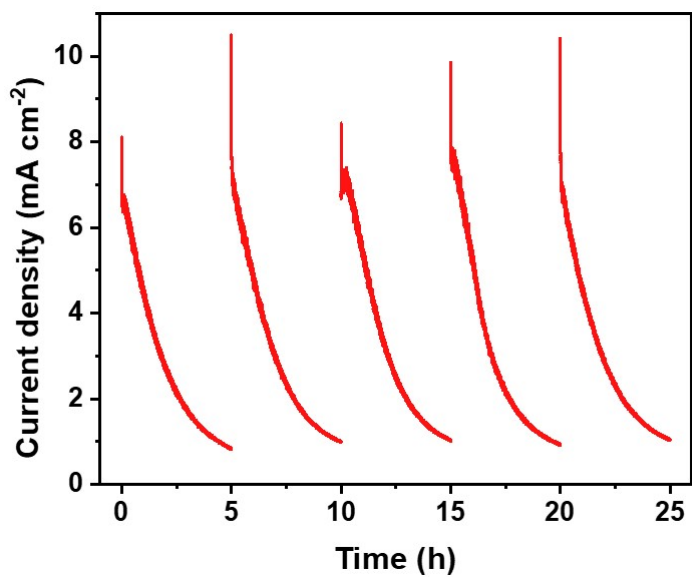


Figure S13. Chronoamperometry experiments of $\text{Ni}_{2.4}\text{S}_{0.1}@\text{CNTs}$ under five successive electrochemical tests for HMFOR.

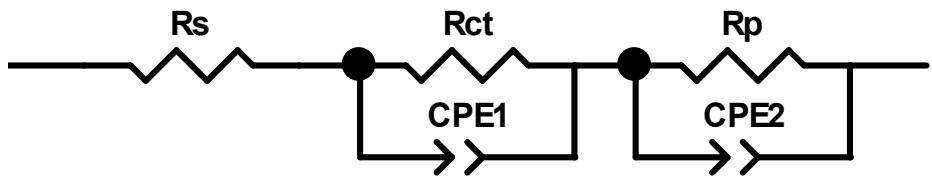


Figure S14. The equivalent circuit used for modeling the measured electrochemical response. The equivalent circuit image. R_s represents the solution resistance, CPE_1 stands for double layer capacitance, the resistance of interface oxidation is denoted as R_{ct} , CPE_2 and R_p are related to the dielectric properties and the resistance of the electrode inner film.

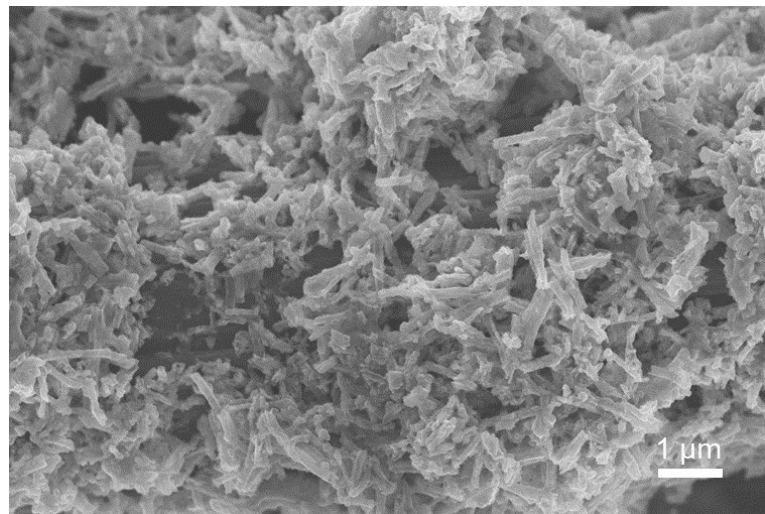


Figure S15. SEM image of the nickel and sulfur co-doped nanotube catalyst after the stability cycle test.

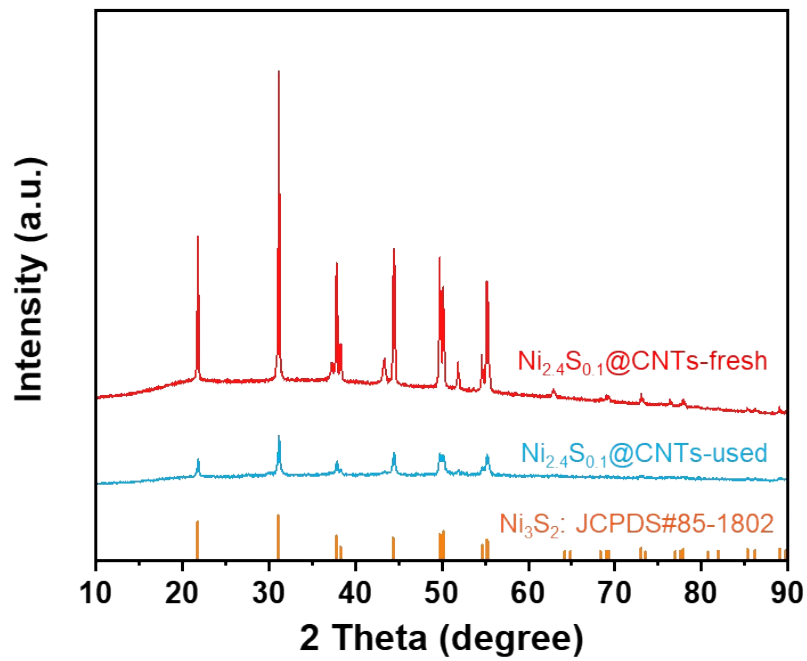


Figure S16. XRD pattern of the nickel and sulfur co-doped nanotube catalyst after the stability cycle test.

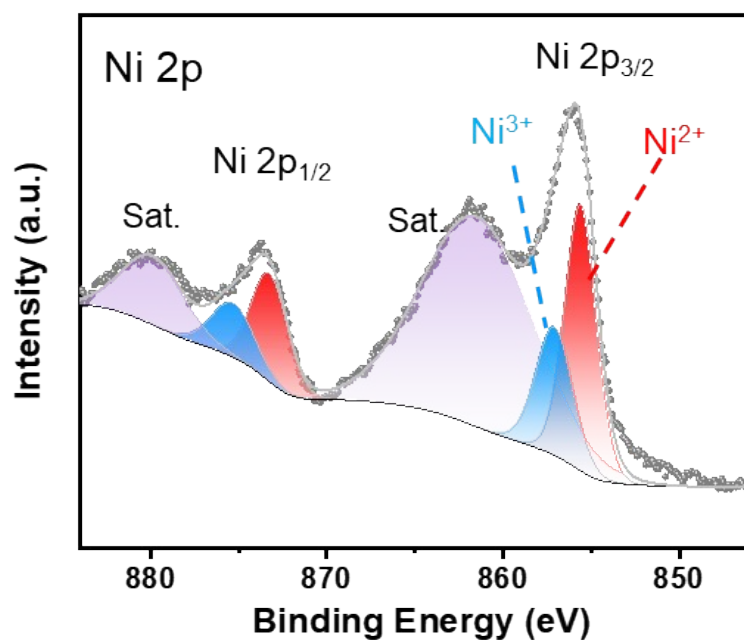


Figure S17. XPS spectrum of the nickel and sulfur co-doped nanotube catalyst after the stability cycle test.

Table S1. Ni contents of $\text{Ni}(\text{NO}_3)_2@\text{CNTs}$, $\text{NiSO}_4@\text{CNTs}$, and $\text{Ni}_{2.4}\text{S}_{0.1}@\text{CNTs}$, determined from ICP-OES measurements.

Samples	Ni wt%
$\text{Ni}(\text{NO}_3)_2@\text{CNT}$	81.1
s	
$\text{NiSO}_4@\text{CNTs}$	62.4
$\text{Ni}_{2.4}\text{S}_{0.1}@\text{CNTs}$	62.7

Table S2. The fitted parameters of Nyquist plots of $\text{Ni}(\text{NO}_3)_2@\text{CNTs}$, $\text{NiSO}_4@\text{CNTs}$ and $\text{Ni}_{2.4}\text{S}_{0.1}@\text{CNTs}$ electrodes.

Samples	R_{ct} (Ω)	R_s (Ω)	C_{dl} (F)
$\text{Ni}(\text{NO}_3)_2@\text{CNT}$	3.67	4.13	0.0033
s			
$\text{NiSO}_4@\text{CNTs}$	2.52	5.23	0.0068
$\text{Ni}_{2.4}\text{S}_{0.1}@\text{CNTs}$	2.02	4.93	0.0063

Table S3. The resistance of each component for $\text{Ni}_{2.4}\text{S}_{0.1}@\text{CNTs}$ in 0.1 M KOH with 10 mM HMF.

Potential (V)	R_s (Ω)	R_{ct} (Ω)	R_p (Ω)
1.25	3.530	79.73	1435
1.30	3.532	69.35	1057
1.35	3.547	60.36	483.7
1.40	3.995	4.492	53.70
1.45	4.107	2.013	26.19
1.50	4.126	1.489	13.66
1.55	4.149	1.223	10.02
1.60	4.207	1.169	5.768
1.65	4.361	1.410	3.777
1.70	4.215	2.107	5.563

Table S4. Performance of $\text{Ni}_{2.4}\text{S}_{0.1}@\text{CNTs}$ catalyst developed in this work (*) and reported materials for oxidation of 5-hydroxymethylfurfural (HMF) to 2,5-furandicarboxylic acid (FDCA).

Electrode Material	HMF conc (mM)	Applied potential (V vs. RHE)	FDCA yield (%)	FE of FDC A (%)	Ref.
$\text{Ni}_{2.4}\text{S}_{0.1}@\text{CNTs}$	10	1.51	~96	~99	This work
$\text{Ni}_{0.9}\text{Cu}_{0.1}(\text{OH})_2$	5	1.45	91.2	91.2	<i>J. Mater. Chem. A</i> , 2021, 9 , 9685-9691. ^[1]
Nanocrystalline Cu	5	1.69	96.4	95	<i>ACS Catal.</i> , 2018, 8 , 1197-1206. ^[2]
P-HEOs/CP	10	1.50	97.4	96.6	<i>Angew. Chem. Int. Ed.</i> , 2021, 60 , 20253-20258. ^[3]
NiCo_2O_4	5	1.50	72	80	<i>Appl. Catal., B</i> , 2019, 242 , 85-91. ^[4]
NiO-CMK-1	20	1.73	-	51.4	<i>Adv. Sustainable Syst.</i> , 2020, 4 , 1900151. ^[5]
NiCoFe-LDHs	10	1.52	~82	-	<i>ACS Catal.</i> , 2020, 10 , 5179-5189. ^[6]
NiCoBDC-NF	10	1.55	99	78.8	<i>J. Mater. Chem. A</i> , 2020, 8 , 20386-20392. ^[7]
$\text{Ni}_{0.5}\text{Co}_{2.5}\text{O}_4$	50	1.45	92.4	90.3	<i>ACS Catal.</i> , 2022, 12 , 4242-4251. ^[8]
Pt/ $\text{Ni}(\text{OH})_2$	50	1.61	98.7	99	<i>Angew. Chem. Int. Ed.</i> , 2021, 60 , 22908-22914. ^[9]
CuO-PdO	50	1.41	96.2	93.7	<i>Adv. Mater.</i> , 2022, 34 , 2204089. ^[10]

Reference

1. J. Zhang, P. Yu, G. Zeng, F. Bao, Y. Yuan and H. Huang, *J. Mater. Chem. A*, 2021, **9**, 9685-9691.
2. D.-H. Nam, B. J. Taitt and K.-S. Choi, *ACS Catal.*, 2018, **8**, 1197-1206.
3. K. Gu, D. Wang, C. Xie, T. Wang, G. Huang, Y. Liu, Y. Zou, L. Tao and S. Wang, *Angew. Chem. Int. Ed.*, 2021, **60**, 20253-20258.
4. M. J. Kang, H. Park, J. Jegal, S. Y. Hwang, Y. S. Kang and H. G. Cha, *Appl. Catal., B*, 2019, **242**, 85-91.
5. F. J. Holzhäuser, T. Janke, F. Öztas, C. Broicher and R. Palkovits, *Adv. Sustainable Syst.*, 2020, **4**, 1900151.
6. M. Zhang, Y. Liu, B. Liu, Z. Chen, H. Xu and K. Yan, *ACS Catal.*, 2020, **10**, 5179-5189.
7. M. Cai, Y. Zhang, Y. Zhao, Q. Liu, Y. Li and G. Li, *J. Mater. Chem. A*, 2020, **8**, 20386-20392.
8. Y. Lu, T. Liu, Y.-C. Huang, L. Zhou, Y. Li, W. Chen, L. Yang, B. Zhou, Y. Wu, Z. Kong, Z. Huang, Y. Li, C.-L. Dong, S. Wang and Y. Zou, *ACS Catal.*, 2022, **12**, 4242-4251.
9. B. Zhou, Y. Li, Y. Zou, W. Chen, W. Zhou, M. Song, Y. Wu, Y. Lu, J. Liu, Y. Wang and S. Wang, *Angew. Chem. Int. Ed.*, 2021, **60**, 22908-22914.
10. P. Zhou, X. Lv, S. Tao, J. Wu, H. Wang, X. Wei, T. Wang, B. Zhou, Y. Lu, T. Frauenheim, X. Fu, S. Wang and Y. Zou, *Adv. Mater.*, 2022, **34**, 2204089.